5798–5809 *Nucleic Acids Research, 2015, Vol. 43, No. 12* *Published online 18 May 2015*
doi: 10.1093/nar/gkv504

Mutations in the CRE pocket of bacterial RNA polymerase affect multiple steps of transcription

Ivan Petushkov[1,2], Danil Pupov[1], Irina Bass[1] and Andrey Kulbachinskiy[1,2,*]

[1]Institute of Molecular Genetics, Russian Academy of Sciences, Kurchatov sq. 2, Moscow 123182, Russia and [2]Molecular Biology Department, Biological Faculty, Lomonosov Moscow State University, GSP-1, Leninskie Gory, Moscow 119991, Russia

Received March 21, 2015; Revised May 01, 2015; Accepted May 04, 2015

ABSTRACT

During transcription, the catalytic core of RNA polymerase (RNAP) must interact with the DNA template with low-sequence specificity to ensure efficient enzyme translocation and RNA extension. Unexpectedly, recent structural studies of bacterial promoter complexes revealed specific interactions between the nontemplate DNA strand at the downstream edge of the transcription bubble (CRE, core recognition element) and a protein pocket formed by core RNAP (CRE pocket). We investigated the roles of these interactions in transcription by analyzing point amino acid substitutions and deletions in *Escherichia coli* RNAP. The mutations affected multiple steps of transcription, including promoter recognition, RNA elongation and termination. In particular, we showed that interactions of the CRE pocket with a nontemplate guanine immediately downstream of the active center stimulate RNA-hairpin-dependent transcription pausing but not other types of pausing. Thus, conformational changes of the elongation complex induced by nascent RNA can modulate CRE effects on transcription. The results highlight the roles of specific core RNAP–DNA interactions at different steps of RNA synthesis and suggest their importance for transcription regulation in various organisms.

INTRODUCTION

To perform gene transcription, RNA polymerase (RNAP) should recognize promoters sequence-specifically and the DNA template with low specificity to guarantee smooth and efficient RNA elongation. In bacteria, this dilemma is resolved by using a dedicated promoter specificity factor, the σ subunit of RNAP that binds the catalytic core enzyme of RNAP and brings it to a promoter. The classical view of the transcription cycle suggested that after transcription initiation, the σ subunit dissociates and core RNAP continues RNA synthesis until it encounters a transcription termination signal (reviewed in (1,2)).

Subsequent studies demonstrated that transcription elongation is not a monotonous process and can be interrupted by transcription pauses of various nature. The σ subunit does not necessarily dissociate from core RNAP during transcription initiation and can cause pauses through specific interactions with promoter-like motifs in the transcribed DNA (3). Factor-independent transcription pauses may result from backtracking of the elongation complex (EC) promoted by unfavorable DNA sequences (4). In addition, core RNAP can respond to several types of specific pause-inducing signals that include: (i) consensus (or 'ubiquitous') pauses that are defined by several nucleotides in the transcription bubble and downstream DNA and result from stabilization of the pre-translocated state of the EC; this is the most widespread type of the pauses in *E. coli* that were recently revealed by whole-genome RNA sequencing analyses (5,6); (ii) hairpin-dependent pauses (such as *hisP*) that depend on the formation of a short RNA hairpin in the RNA exit channel of RNAP and participate in coordination of transcription and translation (7,8); (iii) *opsP* pauses that are recognized by RNAP in the nontemplate DNA strand in the transcription bubble and participate in the recruitment of transcription factor RfaH (7,9); and (iv) U-tract-induced pauses that are proposed to play an important role in transcription termination (reviewed in (10)). The molecular details of specific recognition of these signals are not fully understood.

Recent structural studies of transcription initiation complexes of *Thermus thermophilus* RNAP confirmed the principal role of the σ subunit in promoter recognition but unexpectedly revealed that core RNAP also participates in specific recognition of the nontemplate DNA strand around the starting point of transcription (positions −4/+2); this DNA segment was designated CRE (core recognition element) (11–13). In particular, a nontemplate guanine at promoter position +2 (+2G) is inserted into a pocket ('CRE pocket') formed by two segments of the β subunit (ca. 440–455 and 535–555 amino acid residues, the latter segment also known as 'fork-loop 2'; *E. coli* numbering is used un-

*To whom correspondence should be addressed. Tel: +7 499 196 0015; Fax: +7 499 196 0015; Email: akulb@img.ras.ru

less otherwise indicated). The preceding +1 base is rotated and stacked against a tryptophan residue (W183 in *E. coli* RNAP; Figure 1, Supplementary Figures S1 and S2). Several residues from the CRE pocket, including D446, directly interact with the guanine base and mutations of these residues were shown to impair transcription activity of *E. coli* RNAP (Figure 1B) (11). Furthermore, +2G was shown to stimulate the binding of oligonucleotide promoter mimics suggesting the importance of these interactions for promoter recognition by *E. coli* RNAP (11). We independently showed that this RNAP pocket interacts with highly specific single-stranded DNA aptamers, further suggesting its involvement in specific RNAP–DNA interactions (Pupov *et al.*, in preparation). Recently, crystal structures of *E. coli* RNAP-promoter complexes were reported but no specific details of CRE-pocket–DNA interactions could be revealed due to limited resolution of the structures (14).

It was proposed that similar interactions of core RNAP with the DNA template may contribute to recognition of certain pause-inducing signals during transcription elongation (11,15). Curiously, *E. coli* RNAP was demonstrated to form tight contacts with the downstream segment of the nontemplate strand in ECs, with particular preference for a guanine residue, almost two decades ago (16). However, no experimental evidence in support of the stimulatory role of these interactions in pausing was obtained to date. On the contrary, it was demonstrated that interactions of residue D446 from the CRE pocket with nontemplate guanines counteract consensus pausing by promoting forward RNAP translocation (6). The role of RNAP–CRE interactions in other types of transcription pausing has not been tested.

To investigate the functional roles of RNAP–CRE interactions at various steps of transcription, we obtained RNAPs with point amino acid substitutions and deletions in the CRE pocket. Analysis of their transcription properties confirmed that RNAP–CRE interactions are important for promoter recognition and demonstrated that they also contribute to a certain type of the pausing during transcription elongation.

MATERIALS AND METHODS

Proteins and DNA templates

Mutant variants of the *E. coli rpoB* gene were obtained by site-directed polymerase chain reaction (PCR)-mutagenesis in the pIA545 plasmid and recloned into the pIA679 expression vector encoding all four core RNAP subunits (with a His_6-tag in the N-terminus of the β subunit) (17). The Δ443–451 mutant was obtained by D. Esyunina. Wild-type and mutant *E. coli* core RNAPs were expressed and purified from *E. coli* BL21(DE3) cells as described (17). For *in vivo* experiments, mutant *rpoB* alleles were cloned into the pBAD HisB vector under the control of arabinose-inducible promoter. *E. coli* σ^{70} subunit was obtained as described previously (18). *E. coli nusA* gene was amplified from genomic DNA and cloned into the pLATE52 vector. NusA containing an N-terminal His_6-tag was expressed in *E. coli* BL21(DE3) cells and purified using Polymin P precipitation and Ni-affinity chromatography.

DNA fragments containing wild-type and mutant variants of T7A1 and *rrnB* P1 promoters were obtained by PCR using synthetic template and primer oligonucleotides; the *rrnB* P1* promoter contained a -7G substitution that stabilizes promoter complexes (19). T7A1 promoter followed by λ tR2 terminator was obtained as in (20). DNA template containing a fragment of the *E. coli rpoB* gene fused to the λ P_R promoter for measurements of elongation rates was described previously (21). DNA templates for analysis of *hisP* pausing were obtained by PCR from plasmid pIA226 containing λ P_R promoter followed by the *hisP* site. DNA template for analysis of *opsP* pausing was amplified with synthetic oligonucleotides, cloned into the pGEM-T vector, and the required DNA fragment was obtained by PCR. All promoter sequences are shown in Supplementary Figure S3.

In vitro transcription

For analysis of promoter complex stabilities, holoenzyme RNAPs (50 nM wild-type or mutant core RNAP plus 250 nM σ^{70} subunit) were incubated with promoter DNA (25 nM) in transcription buffers containing 40 mM Tris-HCl, pH 7.9 and 10 mM $MgCl_2$ with addition of 40 mM or 10 mM KCl for T7A1 and *rrnB* P1* promoters, respectively, for 10 min at 37°C. Heparin was added to 100 μg/ml and the samples were incubated for different time intervals, followed by the addition of nucleotide substrates: CpA (25 μM) and uridine triphosphate (UTP) (1 μM, with the addition of α-[^{32}P]-UTP) for wild-type T7A1; CpA (25 μM) and guanosine triphosphate (GTP) (1 μM, with the addition of α-[^{32}P]-GTP) for T7A1+2G; CpA, cytidine triphosphate (CTP) (25 μM) and UTP (1 μM, α-[^{32}P]-UTP) for *rrnB* P1*; CpA, GTP (25 μM) and UTP (1 μM, α-[^{32}P]-UTP) for *rrnB* P1*+2G. The reactions were stopped after 1 min by the addition of stop-solution (8M urea, 20 mM EDTA), RNA products were separated by 23% Polyacrylamide gel electrophoresis (PAGE) and quantified by phosphorimaging using Typhoon 9500 scanner (GE Healthcare). The kinetics of the abortive synthesis decay was fit to single-exponential equation: $A = A_0 \times \exp(-k_{obs} \times t)$, where A is RNAP activity, A_0 is RNAP activity at zero time point (in the absence of heparin) and k_{obs} is the observed rate constant for promoter complex dissociation.

For analysis of *hisP* pausing on the λP_R-*hisP* template, ECs stalled at the +26 promoter position were obtained by incubating preformed promoter complexes of wild-type or mutant RNAPs with a limited substrate set (25 μM ApU, 10 μM adenosine triphosphate (ATP) and GTP, 2.5 μCi α-[^{32}P]-UTP) for 7 min at 37°C. Transcription was restarted by the addition of ATP, UTP (100 μM) and CTP (10 μM). Analysis of *opsP* pausing was performed on the λP_R-*opsP* template in a similar way. ECs were stalled at promoter position +28, followed by the addition of ATP, UTP (100 μM), CTP (20 μM) and GTP (10 μM). The reactions were stopped after increasing time intervals, and RNA products were analyzed by 15% denaturing PAGE, followed by phosphorimaging. Pause efficiencies were calculated as ratios of paused RNAs to the sum of paused and run-off RNA bands, and the data were fit to the single-exponential equation.

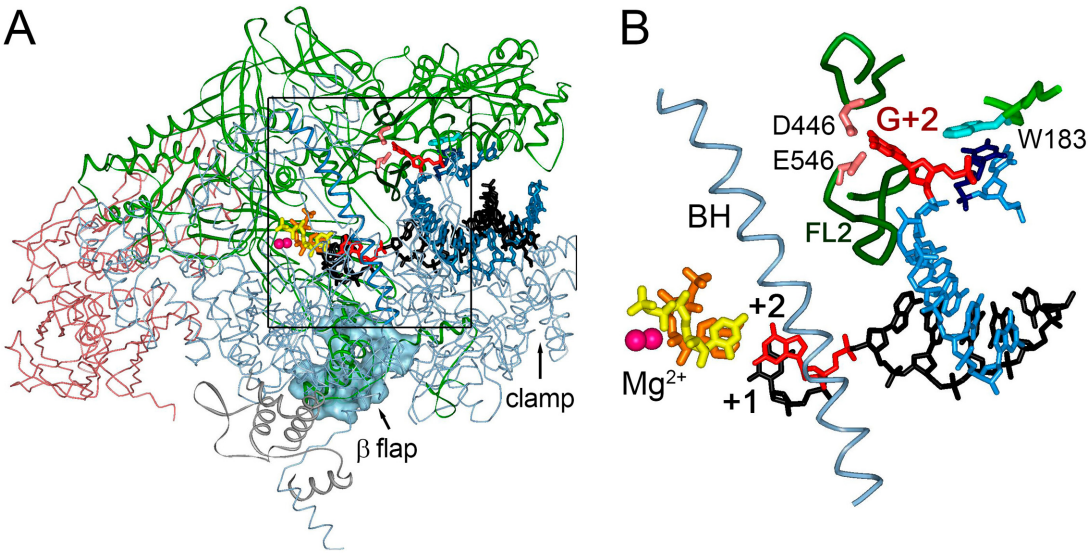

Figure 1. RNAP–CRE interactions in the open promoter complex. (**A**) Structure of *T. thermophilus* RNAP with a promoter DNA fragment (4Q4Z, (13)). The β flap and β′ clamp domains are indicated. The σ subunit is not shown. (**B**) RNAP–DNA interactions at the downstream edge of the transcription bubble. The active site Mg^{2+} ions are shown as purple spheres; the +1 and +2 initiating nucleotides are shown in orange and yellow, respectively. The template and nontemplate DNA strands are black and blue, respectively; DNA nucleotides at promoter position +2 are shown in red, nontemplate thymine at position +1 is dark blue. β subunit segments forming the CRE pocket are shown in green (168–176; 443–451; 533–546, *E. coli* numbering); residues W183, D446 and E546 are shown as stick models.

Analysis of *hisP* pausing on synthetic oligonucleotide scaffolds was performed as described in (22) with modifications. RNA oligonucleotide was 5′-labeled with γ-[^{32}P]-ATP and T4 polynucleotide kinase and mixed with the template DNA strand in transcription buffer (40 mM Tris-HCl, pH 7.9, 10 mM $MgCl_2$, 40 mM KCl) at final concentrations of 500 and 600 nM, respectively. The samples were incubated for 2 min at 95°C and cooled down to 25°C at about 1°C/min. The samples were supplemented with core RNAP (800 nM) and incubated for 15 min at 37°C. Nontemplate DNA oligonucleotide was added (1 μM), the incubation was continued for another 15 min and the samples were diluted 10-fold with the transcription buffer. Antisense RNA (asRNA) oligonucleotide was added to 2 μM when required and incubated for 10 min at 37°C. CTP, UTP and GTP were added to 2 μM and the reaction was stopped after increasing time intervals. A control chase reaction was performed with 500 μM of CTP, UTP and GTP to reveal a background fraction of the complexes that were irreversibly stalled at the pause site. RNA products were analyzed by 19% denaturing PAGE. At each time point, the pause efficiency was calculated as the ratio of the paused RNA product to the sum of the paused and read-through products (minus background values measured in the chase reaction). Observed rate constants for the pause decay and corresponding pause half-life times were calculated by fitting the data to the single-exponential equation.

Analyses of elongation rates and transcription termination were performed on the λP_R-*rpoB* and T7A1-λtR2 templates, respectively, essentially as previously described (21). ECs stalled at positions +26 and +20 of the λ P_R and T7A1 promoters were obtained by the addition of corresponding limited substrate sets to preformed promoter complexes at 37°C. For analysis of elongation rates, the samples were transferred to 20°C, transcription was restarted by the addition of all four NTPs (200 μM each) and heparin (15 μg/ml), and the kinetics of full-length RNA synthesis was monitored at 20°C. For analysis of transcription termination, NTPs were added to 10 μM together with heparin (15 μg/ml) and transcription was performed for 5 min at 37°C, resulting in synthesis of 100 nt terminated and 150 nt run-off RNAs. Reactions were terminated by the addition of stop-solution and RNA products were analyzed by 10% denaturing PAGE. Termination efficiencies are shown in percent of RNA transcripts released at the point of termination relative to the sum of terminated and run-off RNAs.

Cell viability assays

For analysis of *in vivo* effects of the *rpoB* mutations, *E. coli* cells of strain RL585 bearing a temperature-sensitive chromosomal *rpoB* allele (23) were transformed with an empty pBAD vector or with pBAD-based plasmids expressing wild-type and mutant *rpoB* alleles under the control of inducible arabinose promoter. The cells were plated on Petri dishes containing LB agar with addition of 2% glucose and 200 μg/ml ampicillin and incubated for 2–4 days at 30°C. Single colonies were grown in 1 ml of liquid LB for 20 h, diluted to $OD_{600} = 0.4$ followed by serial dilutions, put on LB plates containing 0.2% arabinose and 200 μg/ml ampicillin, and incubated for 2–3 days at 30 or 42°C.

Analysis of the effects of the mutations on rifampicin (Rif) sensitivity was performed in *E. coli* strain DH 5α. The cells were transformed with the same plasmids (but without the addition of glucose), single colonies were picked-up and grown overnight, the cultures were diluted to $OD_{600} = 0.4$ and put on LB plates containing 0.2% arabinose, 200 μg/ml ampicillin and 0, 20 or 50 μg/ml Rif. The plates were incubated for 2 days at 37°C.

RESULTS

We obtained the following mutations in the CRE pocket of *E. coli* RNAP (Figure 1B and Supplementary Figure S1): (i) alanine substitutions of residues D446 and E546; residue D446 is directly involved in specific interactions with nontemplate +2G in promoter complexes; residue E546 is adjacent to D446 and can potentially participate in such interactions based on its different positioning in various RNAP structures (11,13,24,25); (ii) alanine substitution of residue W183 that stacks with the +1 nontemplate promoter nucleotide; and (iii) deletions of the two β subunit segments that form the CRE pocket, Δ443–451 (substituted with five glycine residues) and Δ533–546 (substituted with three glycine residues). All mutant variants of the *rpoB* gene were cloned into expression plasmids encoding all core RNAP subunits, and corresponding RNAPs were expressed and purified from *E. coli* cells (see the 'Materials and Methods' section for details).

Effects of CRE pocket mutations on promoter complex stability

We first tested the effects of the RNAP mutations on promoter binding to confirm the proposed role of the CRE pocket in specific DNA recognition. Previously, the +2G residue in the nontemplate DNA strand was shown to increase stability of RNAP complexes with synthetic DNA scaffolds corresponding to the downstream part of the promoter bubble, in comparison with other three nucleotide variants (11). Furthermore, several mutations in the CRE pocket impaired transcription from a strong λ P_R promoter, which forms very stable complexes with RNAP. However, other substitutions, including D446A, had only minor effects on RNAP activity (11). Thus, to highlight the role of the RNAP–CRE interactions in promoter complex formation, we analyzed the effects of the CRE-pocket mutations on the open complex stability using promoters that form less stable complexes with RNAP and their mutant variants with substitutions at position +2.

We found that the +2T→G substitution significantly increased the half-life time of the open promoter complex (RP_o) formed by wild-type RNAP on the T7A1 promoter ($t_{1/2}$ = 260 and 660 s, respectively; Figure 2 and Table 1). Similarly, a +2G variant of the *rrnB* P1* promoter was more stably bound by RNAP than the wild-type +2C promoter ($t_{1/2}$ = 14 and 25 s; Table 1). Therefore, guanine at position +2 increases the stability of complexes formed by RNAP on natural promoters.

We further measured RP_o stabilities for mutant RNAPs with amino acid substitutions and deletions in the CRE pocket. The E546A substitution did not affect promoter complex stability. D446A and W183A substitutions significantly decreased the RP_o half-lives ($t_{1/2}$ = 100 and 49 s for wild-type T7A1 promoter, respectively) and both deletions dramatically destabilized the complex ($t_{1/2}$ < 10 s; Table 1). Similarly, several other mutations in the same regions of the β subunit were previously shown to decrease promoter complex stabilities on various promoters (Supplementary Figure S1, see Discussion) (26–28).

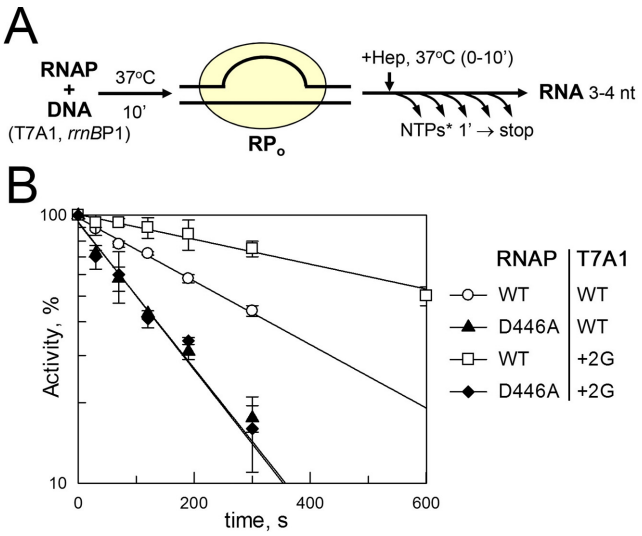

Figure 2. Effects of mutations in the CRE pocket on promoter complex stability. (**A**) Outline of experiment. Heparin was added to preformed promoter complexes, followed by nucleotide addition after increasing time intervals. The reactions were performed with CpA+(UTP/GTP) in the case of T7A1 and CpA+(CTP/GTP)+UTP in the case of *rrnB* P1* promoter variants (with addition of α-[^{32}P]-UTP), resulting in the synthesis of 3 and 4 nt RNA products, respectively. (**B**) Kinetics of promoter complex dissociation for the wild-type and +2G T7A1 promoter variants, measured for wild-type and D446A RNAPs. Averages and standard deviations from two to three independent experiments are shown; the lines correspond to single-exponential fits of the data.

In contrast to wild-type RNAP, the +2T→G substitution in the T7A1 promoter did not increase promoter complex stability in the case of D446A RNAP and only slightly increased it in the case of E546A RNAP (Figure 2B and Table 1). At the same time, promoter complex stability was still increased in the case of the W183A mutant. Therefore, in agreement with structure-based predictions (11), specific interactions of residues D446 and E546 with +2G appear to be involved in stabilization of promoter complexes.

General effects of CRE-pocket mutations on transcription elongation and termination

Our next goal was to reveal the effects of the CRE-pocket mutations on the elongation step of transcription. We first measured average elongation rates for mutant RNAPs using a ∼500 bp *E. coli rpoB* template fused to the λP_R promoter. ECs stalled at the +26 promoter position were chased with all four NTPs and the kinetics of the run-off RNA synthesis was analyzed (Figure 3 and Supplementary Figure S4). The D446A and W183A substitutions did not significantly change the average rate of RNA synthesis, the E546A substitution increased it ∼2-fold, while the Δ443–451 deletion slightly decreased the rate and the Δ533–546 deletion dramatically impaired RNA elongation.

Previously, the D446A substitution was shown to increase consensus (ubiquitous) pausing at most genome positions (6). However, careful inspection of the RNA products synthesized during transcription of the *rpoB* template revealed that this substitution stimulated pausing at some sites (probably, corresponding to consensus pause motifs)

Table 1. Promoter complex stabilities of wild-type and mutant *E. coli* RNAP variants

RNAP	Promoter	$t_{1/2}$ (s)	Rel.
WT	T7A1	257 ± 5	1
	T7A1+2G	662 ± 45	2.6
	rrnB P1*	14 ± 3	1
	rrnB P1*+2G	25 ± 1	1.8
D446A	T7A1	104 ± 9	0.40
	T7A1+2G	107 ± 15	0.42
E546A	T7A1	245 ± 30	0.96
	T7A1+2G	356 ± 13	1.4
W183A	T7A1	49 ± 10	0.19
	T7A1+2G	94 ± 22	0.37
Δ443–451	T7A1	< 10	< 0.04
Δ533–546	T7A1	< 10	< 0.04

Promoter complex half-life times were determined from single exponential fits of the heparin challenge experiment shown in Figure 2. Wild-type (WT) T7A1 and *rrnB* P1 promoters contain T and C at position +2, respectively. A -7G variant of the *rrnB* P1 promoter (*rrnB* P1*) was used to increase promoter complex stability (19). See Supplementary Figure S3 for all promoter sequences. The last column shows $t_{1/2}$ values relative to WT RNAP.

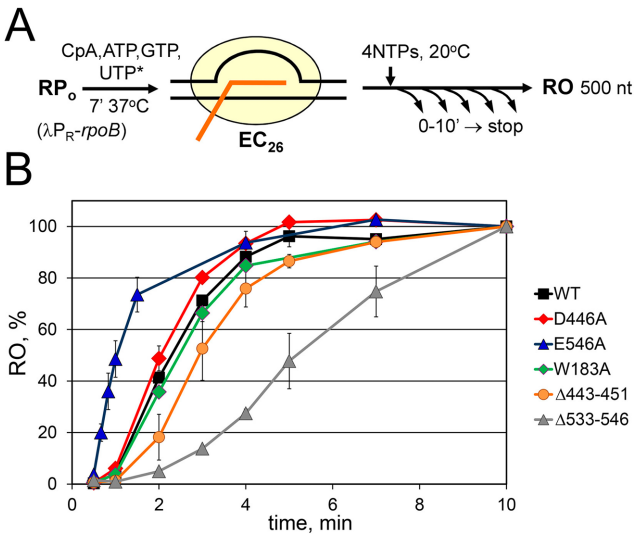

Figure 3. Comparison of elongation rates of mutant RNAPs. (**A**) Outline of experiment. (**B**) Kinetics of accumulation of full-length RNA transcript (in percent of the activity measured at the 10 min time point) for wild-type and mutant RNAP variants (averages and standard deviations from two to three independent experiments).

but decreased it at other template positions, resulting in only minor cumulative change in the average rate of elongation (Supplementary Figure S4). The E546A substitution decreased pausing at most template positions thus explaining the stimulatory effect of this mutation on elongation. In contrast, the 533–546 deletion increased pausing resulting in much slower RNA extension (Supplementary Figure S4).

Since the mutations in the CRE pocket affected the overall rate of elongation, we tested their effects on intrinsic transcription termination, which is known to depend on the rate of RNA synthesis (10). The effects of mutations on termination at the λ tR2 terminator in general inversely correlated with their effects on the rate of elongation. The W183A and Δ443–451 mutations did not significantly change termination. The E546A and Δ533–546 mutations respectively decreased and increased the termination efficiency (Table 2). Interestingly, the D446A substitution,

Table 2. Efficiencies of transcription termination at the λ tR2 terminator by wild-type and mutant RNAPs

RNAP	tR2 (%)	Rel.
WT	50 ± 1	1
D446A	34 ± 1	0.68
E546A	41 ± 3	0.82
W183A	53 ± 6	1.1
Δ443–451	52 ± 5	1.0
Δ533–546	69 ± 3	1.4

The last column shows termination efficiencies relative to wild-type RNAP.

which had only a week effect on the average rate of elongation, significantly suppressed termination suggesting that this residue may have a specific role in this process (Table 2). The termination defects of the D446A and E546A mutants were also observed in the presence of transcription factor NusA which stimulated intrinsic termination by wild-type RNAP to a higher level than termination by the mutant RNAPs (Supplementary Figure S5).

Role of the CRE pocket in hairpin-dependent pausing

The observed effects of the CRE-pocket mutations on transcription elongation and termination prompted us to more thoroughly investigate their effects on transcription pausing which plays essential roles in both processes. We focused on the analysis of the D446A and E546A substitutions that could affect specific recognition of the nontemplate guanine residue in the CRE pocket.

To reveal mechanistic differences in the effects of the CRE-pocket mutations on the recognition of various types of pause signals, we analyzed pausing at two specific pause sites, *hisP* (stabilized by RNA hairpin formation) and *opsP* (stabilized by RNAP interactions with the nontemplate DNA strand) (7). Importantly, both sites share some sequence features with the consensus pause site; in particular, both contain guanine nucleotides at positions immediately downstream of the pause sites (+1G, corresponds to +2G in promoter complexes in respect to the position of the RNAP active site; Figure 4A and Supplementary Figure S7A, see below).

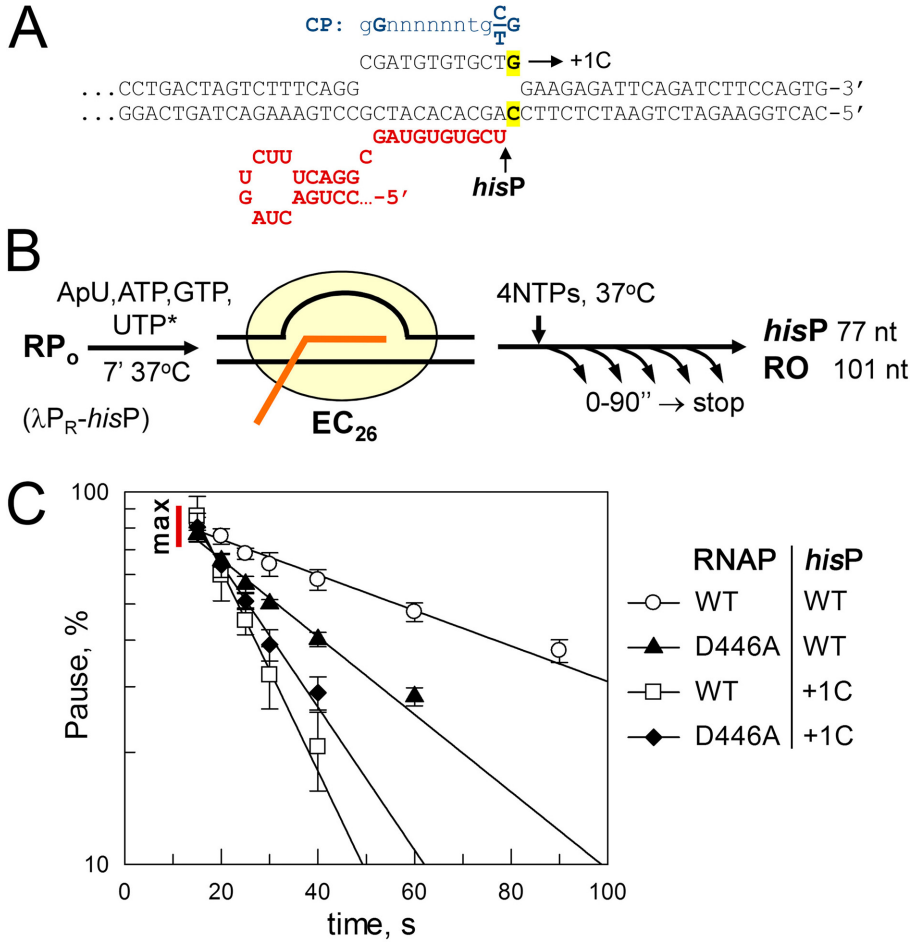

Figure 4. Analysis of hairpin-dependent pausing by wild-type and mutant RNAPs. (**A**) Structure of the *hisP* transcription template. The major pausing position is indicated below the RNA transcript. The consensus pause-inducing sequence (CP) identified in genome-wide experiments is shown in blue in the same register relative to the pause position. +1G is shown in yellow; the +1C template contained a C:G base pair instead of G:C at this position. (**B**) Outline of experiment. (**C**) Kinetics of the pause decay measured on the wild-type and +1C templates for wild-type and D446A RNAPs. Averages and standard deviations from three to four independent experiments are shown; the lines are single-exponential fits of the data.

We first compared pause-inducing properties of wild-type *hisP* site and its variants with substitutions of +1G and +2G with C (cytosine substitutions were chosen to preserve the stability of DNA duplex at corresponding positions). The +1G→C substitution significantly reduced the pause half-life time for wild-type RNAP (from 64.0 to 11.7 s; Figure 4 and Table 3). This agrees with previous reports showing that downstream DNA sequences contribute to hairpin-dependent pausing (29–31). The effect was specific for the +1 position since the +2G→C substitution did not decrease pausing but slightly increased it (∼1.5 fold; Table 3).

Mutations in the CRE pocket had distinct effects on *hisP* pausing. Both the D446A and E546A substitutions significantly decreased the pause half-life times (about 2.5-fold; Table 3). This contrasts previously reported stimulatory effect of the D446A substitution on consensus pausing (6). At the same time, the W183A substitution did not significantly affect pausing ($t_{1/2}$ = 69.5 s), suggesting that this residue does not play an important role in the *hisP* recognition.

We then tested whether RNAPs with mutations of D446 and E546 are responsive to nucleotide substitutions in the *hisP* pause signal. Remarkably, the +1G→C substitution had significantly weaker effects on pausing by mutant RNAPs in comparison with the wild-type enzyme. The pause half-life times were reduced ∼1.8- and 3-fold for the D446 and E546 mutants, in comparison with the 5.5-fold change observed for wild-type RNAP (Figure 4C and Table 3). Again, this effect was specific for the +1 position since the +2G→C substitution did not decrease but stimulated *hisP* pausing by mutant RNAPs to the same extent as in the case of wild-type RNAP (∼1.5-fold; Table 3).

Furthermore, when analyzed on the +1C template, the D446A substitution did not decrease the pause half-life but even increased it in comparison with the wild-type RNAP (13.9 versus 11.7 s; Figure 4C and Table 3). Thus, the deleterious effect of this mutation on pausing at the wild-type *hisP* site can be fully attributed to the loss of interactions of the D446 residue with +1G. Similarly, the E546A substitution had a weaker effect on pausing at the +1C *hisP* site relative to wild-type RNAP (∼1.4-fold versus 2.6-fold differences in the pause half-life times on the wild-type template).

Importantly, neither the +1C substitution nor the D446A mutation significantly affected the pausing efficiency since the maximal pausing, measured at the first time point (15 s,

Table 3. *HisP* half-life times (in seconds) for wild-type and mutant RNAP variants

RNAP	*hisP* WT	*hisP* +1C	*hisP* +2C
WT	64.0 ± 6.4 **1**	11.7 ± 1.9 **0.18**	87.0 ± 1.7 **1.4**
D446A	24.8 ± 1.7 **0.39**	13.9 ± 2.1 **0.22**	36.1 ± 5.5 **0.56**
E546A	24.5 ± 3.1 **0.38**	8.2 ± 1.1 **0.13**	35.1 ± 3.8 **0.55**

The numbers in bold show the $t_{1/2}$ values relative to the value measured for wild-type RNAP on the wild-type *hisP* template.

which roughly corresponds to the time required for RNAP to reach the *hisP* site on this DNA template), was comparable for all reactions (80–85%; Figure 4C). Thus, interactions with +1 guanine are likely important for stabilization of the paused state but not for initial recognition of the pause-inducing signal. Overall, the role of CRE-pocket–DNA interactions in the recognition of the *hisP* signal is apparently different from that in consensus pausing, which is suppressed by these interactions (6).

Role of the RNA hairpin in CRE-dependent pausing

One important difference between consensus and *hisP* pauses is the presence of a folded RNA hairpin in the RNA exit channel of RNAP in the latter case. The hairpin was shown to induce long-range conformational changes in RNAP, resulting in clamp opening and preventing EC translocation ((8,32); see the 'Discussion' section). To understand a possible role of the hairpin in the modulation of the RNAP–CRE response, we employed a recently described oligonucleotide-based pausing assay (8,22). In this assay, EC is assembled on a scaffold based on the *hisP* sequence but lacking the RNA hairpin, followed by addition of NTP substrates, either in the absence or presence of complementary asRNA (Figure 5A and B).

In agreement with published studies (8,22), we found that RNA duplex greatly increases both the pause half-life time ($t_{1/2}$ = 10.6 and 52.8 s in the absence and presence of asRNA, respectively) and the pause efficiency (P_{max} = 58.3 and 85.9%) for wild-type RNAP. Similarly to the wild-type *hisP* template, the D446A mutation decreased the pause half-life in the presence of the RNA duplex (although the effect was less dramatic; $t_{1/2}$ = 34.0 s). In contrast, the same mutation did not decrease but even slightly increased the pause duration in the absence of asRNA ($t_{1/2}$ = 13.3 s; Figure 5C and D). We therefore conclude that the difference in the RNAP response to +1G in the two types of the pause-inducing signals is mediated by the RNA hairpin-induced changes in the EC structure (see the 'Discussion' section).

Since the D446A substitution suppressed *hisP* pausing we proposed that it may promote forward translocation of the paused complex, which was shown to predominantly adopt the pre-translocated state (8,33). To test the effects of the D446A substitution on translocation, we compared the rates of RNA pyrophosphorolysis by wild-type and mutant RNAPs in ECs assembled on the synthetic scaffold and stalled at the pause site (Supplementary Figure S6). Surprisingly, we observed that the D446A substitution increased the reaction rate (Supplementary Figure S6C and D). At the same time, wild-type and D446A RNAPs revealed similar dependencies of the reaction rates on the pyrophosphate concentration (Supplementary Figure S6E) suggesting that the mutation did not significantly affect pyrophosphate binding. Therefore, the mutation might either favor the pre-translocated EC conformation or facilitate the pyrophosphorolysis reaction in the RNAP active center (see the 'Discussion' section).

Effect of the D446A substitution on o*psP* pausing

We next analyzed RNAP pausing at the *opsP* site, a 12-nt sequence motif that also has similarities with the consensus pause motif and induces pausing at two positions, before the last nucleotide of the site and one nucleotide downstream of it (Supplementary Figure S7). Both pausing positions are followed by guanines in the nontemplate strand, suggesting that they might also be recognized by the CRE pocket of RNAP. However, in contrast to the *hisP* signal, no RNA hairpin is formed during pausing at the *opsP* site.

Comparison of the pausing kinetics for wild-type and D446A RNAPs revealed that the mutation significantly stimulated pausing at the upstream position (37P in Supplementary Figure S7C and D) and had essentially no effect on downstream pausing (39P). This contrasts *hisP*-pausing that is suppressed by the D446A substitution. The mechanism of the 37P pause may therefore be similar to consensus pausing (in accord with the sequence similarities between these two sites, Supplementary Figure S7A) that is also stimulated by the D446A substitution (6). At the same time, the mechanism of pausing at the 39P site may be different; indeed, a significant fraction of the downstream paused complex was shown to enter a backtracked state, susceptible to Gre-induced RNA cleavage (34).

In vivo effects of the CRE-pocket mutations

Finally, we tested whether the mutant RNAP variants can support cell growth when introduced into a temperature-sensitive *E. coli* strain with defects in expression of chromosomal *rpoB* allele (RL585; (23)). Expression of wild-type plasmid-encoded *rpoB* restores the growth of this strain under restrictive conditions (at 42°C; Figure 6A). The D446A and E546A mutants are also viable suggesting that these mutations do not dramatically perturb cellular RNAP function. At the same time, deletions in the CRE pocket (Δ443–451 and Δ533–546) do not support cell growth under these

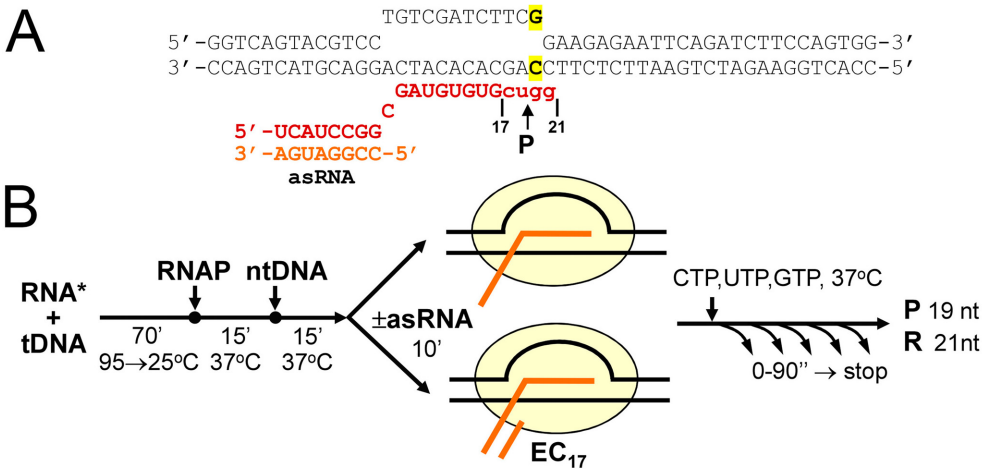

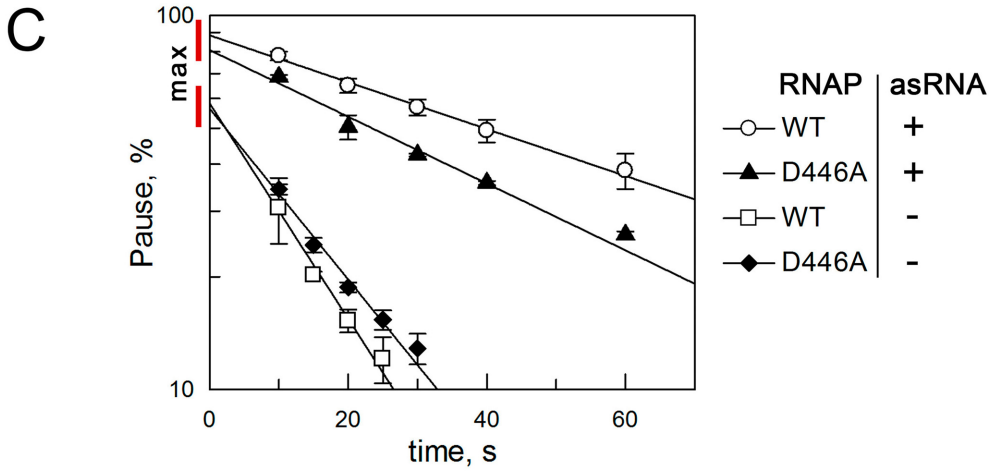

D

RNAP	$t_{1/2}$ (s)		P_{max} (%)	
	-oligo	+oligo	-oligo	+oligo
WT	10.6 ± 2.5	52.8 ± 5.1	58.3 ± 12.0	85.9 ± 1.8
D446A	13.3 ± 1.2	34.0 ± 0.9	56.3 ± 5.2	81.3 ± 0.7

Figure 5. Role of RNA duplex in RNAP pausing at the *hisP* site. (**A**) Structure of the scaffold template used in the experiments. RNA is red, with the four 3′-terminal nucleotides added during transcription shown in lowercase letters. Positions of the 3′-end in the starting, paused and read-through (R) transcripts are indicated. Antisense RNA (asRNA) oligonucleotide is orange. The +1 G:C base pair is shown in yellow. (**B**) Outline of experiment. (**C**) Pausing kinetics measured in the absence or presence of asRNA for wild-type and D446A RNAPs. (**D**) Pause half-life times and pause efficiencies (P_{max}, predicted pausing at zero time point) determined from the pause decay curves.

conditions. Moreover, the cells containing these *rpoB* alleles revealed pronounced growth defects even at permissive temperature (30°C) (Figure 6B) suggesting that both deletions are toxic when expressed *in vivo*.

The CRE pocket is located close to the Rif pocket also formed by the β subunit, and some mutations of Rif resistance were mapped within fork-loop2 and adjacent regions (Supplementary Figure S1). We therefore tested the effects of the mutations in the CRE pocket on Rif resistance of a sensitive *E. coli* DH5α strain. Expression of the wild-type, D446A and E546 β subunit variants did not change its Rif sensitivity (Figure 6B). Surprisingly, however, the Δ533–546 cells could grow at elevated Rif concentrations (50 μg/ml) demonstrating that RNAP with this deletion can support cell growth despite its toxicity in the RL585 strain (see above) (Figure 6A). The observed differences may be likely explained by the decreased viability of the temperature-sensitive RL585 strain (23). The Δ443–451 cells also revealed low level of Rif resistance (20 μg/ml). The resistance of these deletion alleles of *rpoB* is consistent with the localization of some known Rif-resistance mutations in the deleted regions (amino acid substitutions at positions 447, 448, 533, 534, 536, 537; deletions Δ531–533, Δ535–542; Supplementary Figure S1) (26,35–38) and the involvement of fork-loop2 in direct interactions with Rif (35,36).

DISCUSSION

Our results suggest that sequence-specific interactions of the core enzyme of bacterial RNAP with the downstream edge of the transcription bubble play important roles at dif-

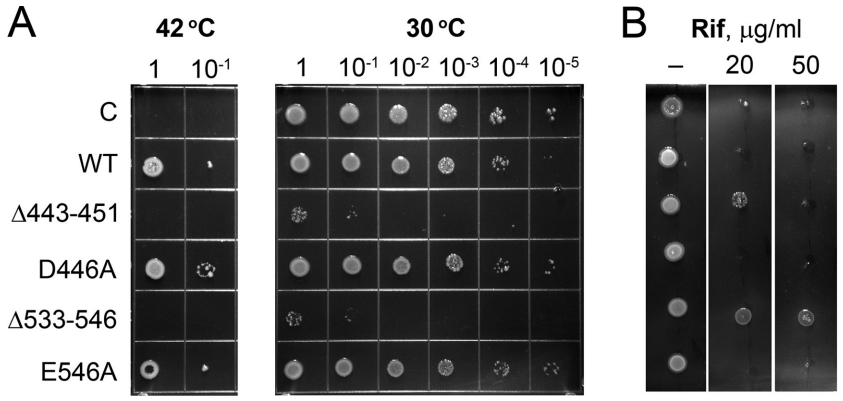

Figure 6. *In vivo* analysis of the effects of CRE pocket mutations on cell viability and Rif resistance. (**A**) *E. coli* temperature-sensitive strain RL585 was transformed with plasmids bearing inducible copies of wild-type and mutant *rpoB* genes or a control plasmid (first row) and grown at either restrictive (left) or permissive (right) temperature. (**B**) The same plasmids were transformed into *E. coli* strain DH5α and the cells were grown at 37°C in the absence or presence of Rif.

ferent steps of transcription and, in particular, make different contributions to different types of transcription pausing. The roles of these interactions in transcription is illustrated in Figure 7. As is shown in the figure, the active center of RNAP contains two functional sites, *i* and *i+1* that accommodate the NTP and RNA substrates during transcription, and can adopt two principal conformations, pre- and post-translocated. In the RP_o, the *i* and *i+1* sites bind the two initiating NTPs corresponding to promoter positions +1 and +2, respectively. Similarly, in the post-translocated EC these sites accommodate the 3′-end of RNA and the incoming NTP (at position +1 relative to the RNA 3′-end). Following nucleotide addition, EC occurs in the pre-translocated conformation in which both sites are occupied by nascent RNA. Available data suggest that the interactions of the CRE pocket with the nontemplate DNA strand can affect the conformational state of the RNAP active center and EC translocation.

During promoter recognition, the nontemplate +2G base, if present in the promoter sequence, can be accommodated in the CRE pocket and this increases the open complex stability (Figure 7A; (11) and this work). Residues D446 and E546 likely make direct contribution to these interactions since their substitutions abolish the stimulating effect of the +2G residue on promoter binding. The +2G position in promoter complexes corresponds to the *i+1* site of the RNAP active center that accommodates the +2 NTP substrate. Thus, such interactions may also play a role in positioning of the template DNA strand in the correct register. In addition, the CRE pocket as a whole plays an important role in the RP_o formation since many mutations in this region including those studied in this work destabilize RNAP-promoter complexes, and some of them mimic the effects of small alarmone ppGpp and its cofactor DksA on transcription (Supplementary Figure S1, (26–28,39)). This may be explained by the loss of favorable interactions of this pocket with the nontemplate DNA strand. Indeed, previously studied deletion Δ436–445 in the *E. coli* β subunit, which overlaps with the Δ443–451 deletion studied in this work, was shown to impair melting of the downstream part of the transcription bubble around the starting point of transcription, likely due to the loss of RNAP–DNA interactions in this region (28). Substitution of residue W183, which is conserved in most bacteria (Supplementary Figure S1), also destabilizes promoter complexes suggesting that its stacking interactions with the +1 nontemplate nucleotide observed in the X-ray structures are important for open complex formation. Interestingly, recent analysis of the effects of several W183 mutations on transcription initiation by *E. coli* σ^{54} holoenzyme RNAP revealed no defects in promoter complex stability but suggested that this residue is involved in initial steps of RNA synthesis and RNAP translocation (40). It remains to be established whether it might play similar roles during transcription initiation by the σ^{70} holoenzyme.

During transcription elongation, the interactions of the CRE pocket with the DNA template likely modulate transcription pausing. Depending on the type of the pause, these interactions can either suppress or stimulate RNA elongation. In the case of the consensus pauses, which are stabilized in the pre-translocated state because of an unfavorable DNA sequence (5,6), the binding of the +1G in the CRE pocket was proposed to stimulate forward RNAP translocation by stabilizing the post-translocated EC conformation (Figure 7B and C). Interestingly, +1G by itself promotes pausing and prevents RNAP translocation, likely because the G:C base pair is more difficult to melt when present in the *i+2* position in the pre-translocated complex, and the template C is poorly accommodated in the *i+1* site after translocation (41). Similarly, *opsP* pausing, which is dependent on the nontemplate DNA strand recognition, may be alleviated by the interactions of the CRE pocket with nontemplate guanine immediately downstream of one of the two major pausing positions (Supplementary Figure S7).

In contrast to the previously proposed antipausing role of the RNAP–CRE interactions (6), these interactions stimulate hairpin-induced pausing, which also occurs in the pre-translocated EC conformation (8,33). In particular, we demonstrated that substitutions of residues D446 and E546 in the CRE pocket significantly decrease the pause half-lives, depending on the presence of +1G in the pause se-

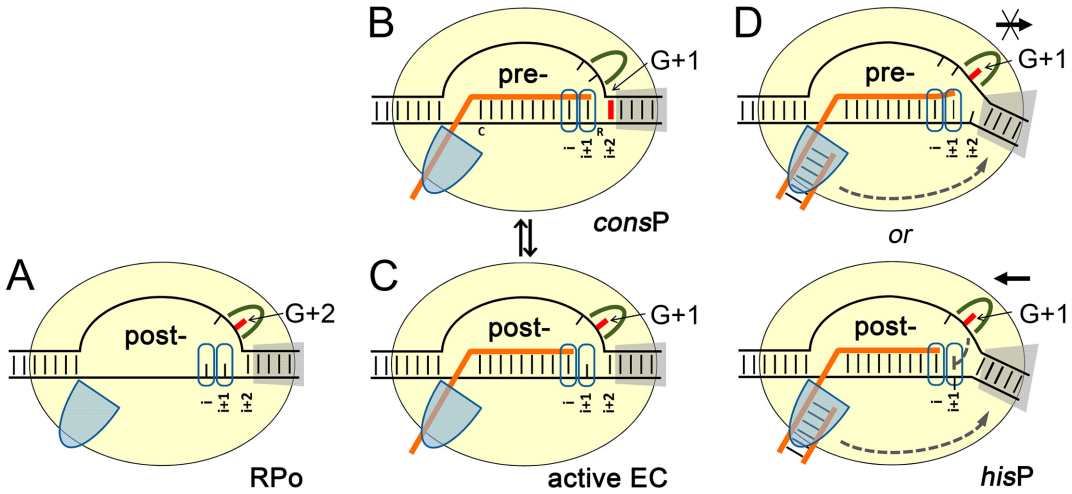

Figure 7. CRE–RNAP interactions at different steps of transcription. RNAP is schematically shown as a yellow oval; the CRE pocket is green; the β flap is shown as a blue semi-oval; the downstream DNA binding channel is gray; the nontemplate guanine downstream of the active site is red. The *i*, *i+1* and *i+2* positions are indicated. (**A**) +2G bound in the CRE pocket stabilizes the open promoter complex. (**B**) Consensus pause complexes are stabilized in the pre-translocated conformation defined by several conserved nucleotides, including a G:C pair at the upstream boundary of the RNA:DNA hybrid, pyrimidine:purine pair (Y:R) in the *i+1* site and a G:C pair downstream of the active site. (**C**) Interactions of +1G with the CRE pocket promote forward EC translocation and suppress consensus pausing. (**D**) RNA hairpins or duplexes formed in the RNA exit channel modulate the effects of +1G/CRE-pocket interactions, likely through changes in the clamp conformation and positions of the downstream duplex and the nontemplate DNA strand. This results in stabilization of the paused state, either by preventing EC translocation (upper) or by inhibiting nucleotide addition in the post-translocated state (lower).

quence. Furthermore, we showed that these effects are strictly dependent on the RNA duplex formation in the RNA exit channel of RNAP. Previously, the RNA hairpin, which folds under the flap domain of RNAP, was shown to increase the pause half-life by inducing clamp-opening and preventing the trigger loop folding in the active center and RNAP translocation (8,32). In addition, the RNA 3′-end in the paused complex was proposed to adopt a frayed conformation in the *i+1* site, thus preventing its further extension (33). We speculate that these conformational changes might modulate the effects of +1G on pausing in two alternative ways.

First, clamp opening and associated changes during pausing alter the position of the downstream DNA duplex (15) and may also change the path of the nontemplate DNA strand in the melted region, thus allowing +1G to be melted and accommodated in the CRE pocket in the pre-translocated state of the EC; this may impede RNAP translocation (Figure 7D, upper). At the same time, recent direct measurements of the downstream DNA melting demonstrated that +1G in the *hisP* site preferentially adopts a base-paired conformation thus suggesting that such melting may occur only transiently (8).

Second, +1G may be bound in the CRE pocket in the post-translocated EC conformation that may be transiently formed in the paused complex. This binding may help to prevent NTP addition in the *i+1* site by affecting the conformation of the adjacent elements of the active center (Figure 7D, lower), including the trigger loop and the bridge helix, which directly contacts the flexible fork-loop 2 region forming a part of the CRE pocket (Figure 1B). The EC in the elemental paused state, which is proposed to precede other pausing events, was shown to adopt a post-translocated conformation in which the *i+1* site is partially occluded by the kinked bridge helix (15). The interactions of +1G with the CRE pocket may contribute to such unproductive conformation thus favoring backward RNAP translocation over nucleotide addition. In support of this idea, our data on stimulation of pyrophosphorolysis at the pause site by the D446A substitution suggest that in wild-type RNAP the interactions of residue D446 with +1G actually promote forward RNAP translocation, similarly to consensus pausing. However, in contrast to consensus pausing, the hairpin formation likely stabilizes inactive active center conformation and shifts the equilibrium toward the pre-translocated state with frayed RNA (8,15).

The CRE pocket also likely plays a general role in transcription elongation since CRE-pocket mutations significantly affected the rate of RNA synthesis by bacterial and eukaryotic RNAPs ((42,43) and this work). Furthermore, β subunit substitutions D444G and H447R in the CRE pocket in *E. coli* RNAP were proposed to destabilize transcription complexes during transcription-replication collisions (44). We observed that the D446A substitution decreased *hisP* pausing but stimulated other types of transcription pauses (see above). At the same time, the E546A substitution suppressed most transcription pauses suggesting that this residue may contribute to various types of pausing through direct contacts with DNA (as proposed for *hisP* pausing) and/or by affecting the fork-loop 2 conformation. The most dramatic changes in RNA elongation were observed in the case of the Δ533–546 deletion that significantly increased transcription pausing. The observed effects can be explained by either changes in RNAP interactions with the nontemplate DNA strand or indirect effects of the mutations on the active site conformation (see above).

The mutations in the CRE pocket also affected intrinsic transcription termination, probably as a result of al-

tered pausing; indeed, the termination effects of the mutations correlated with their effects on hairpin-dependent pausing. In particular, suppression of termination by the D446A and E546A substitutions indicates that contacts of these residues with DNA may be important for termination-associated pausing and/or subsequent EC dissociation. It remains to be established whether the RNAP–CRE interactions may play a stimulatory or an inhibitory role in the case of other types of transcription pauses and related regulatory events, including factor-dependent pausing and termination.

Given considerable level of evolutionary conservation of the CRE pocket (Supplementary Figure S1), its regulatory functions in DNA recognition likely extend to eukaryotic homologs of bacterial RNAP. In particular, it was noted that *S. cerevisiae* RNAPII can also accommodate a non-template base in this pocket (Supplementary Figure S2C) (11,45). Mutations in the fork-loop 2 region in *S. cerevisiae* RNAPII were shown to affect RNAP interactions with downstream DNA and EC translocation (42). Furthermore, substitution D370A in the second largest subunit of *S. cerevisiae* RNAPIII was shown to decrease termination (46), similarly to the equivalent D446A substitution in *E. coli* RNAP.

In accordance with their significant effects on various steps of transcription, many studied mutations in the CRE pocket have pronounced *in vivo* phenotypes including changes in stringent response and antibiotic sensitivity (this work, (26,27,37)). Even the Δ533–546 deletion that revealed dramatic changes in promoter binding, RNA elongation and termination, and was toxic under certain conditions *in vivo* could nevertheless confer Rif-resistance to the bacterial cells. Thus, the CRE pocket is an evolvable RNAP determinant that plays important roles in transcription regulation and antibiotic resistance and may be a target for rational design of RNAP variants with altered DNA specificities.

SUPPLEMENTARY DATA

Supplementary Data are available at NAR Online.

ACKNOWLEDGEMENTS

We thank D. Esyunina for help with cloning and protein purification, R. Landick for helpful discussions and suggestions on the pausing assays, I. Artsimovitch for strains, plasmids and discussions, and D.G. Vassylyev for structure-based suggestions on the positions of the β subunit substitutions.

FUNDING

Russian Academy of Sciences Presidium Program in Molecular and Cellular Biology; Russian Foundation for Basic Research [14–04–01696, 14–04–32029].
Conflict of interest statement. None declared.

REFERENCES

1. Haugen,S.P., Ross,W. and Gourse,R.L. (2008) Advances in bacterial promoter recognition and its control by factors that do not bind DNA. *Nat. Rev. Microbiol.*, **6**, 507–519.
2. Feklistov,A., Sharon,B.D., Darst,S.A. and Gross,C.A. (2014) Bacterial sigma factors: a historical, structural, and genomic perspective. *Annu. Rev. Microbiol.*, **68**, 357–376.
3. Perdue,S.A. and Roberts,J.W. (2011) Sigma(70)-dependent Transcription Pausing in Escherichia coli. *J. Mol. Biol.*, **412**, 782–792.
4. Nudler,E. (2012) RNA polymerase backtracking in gene regulation and genome instability. *Cell*, **149**, 1438–1445.
5. Larson,M.H., Mooney,R.A., Peters,J.M., Windgassen,T., Nayak,D., Gross,C.A., Block,S.M., Greenleaf,W.J., Landick,R. and Weissman,J.S. (2014) A pause sequence enriched at translation start sites drives transcription dynamics in vivo. *Science*, **344**, 1042–1047.
6. Vvedenskaya,I.O., Vahedian-Movahed,H., Bird,J.G., Knoblauch,J.G., Goldman,S.R., Zhang,Y., Ebright,R.H. and Nickels,B.E. (2014) Transcription. Interactions between RNA polymerase and the 'core recognition element' counteract pausing. *Science*, **344**, 1285–1289.
7. Artsimovitch,I. and Landick,R. (2000) Pausing by bacterial RNA polymerase is mediated by mechanistically distinct classes of signals. *Proc. Natl. Acad. Sci. U.S.A.*, **97**, 7090–7095.
8. Hein,P.P., Kolb,K.E., Windgassen,T., Bellecourt,M.J., Darst,S.A., Mooney,R.A. and Landick,R. (2014) RNA polymerase pausing and nascent-RNA structure formation are linked through clamp-domain movement. *Nat. Struct. Mol. Biol.*, **21**, 794–802.
9. Artsimovitch,I. and Landick,R. (2002) The transcriptional regulator RfaH stimulates RNA chain synthesis after recruitment to elongation complexes by the exposed nontemplate DNA strand. *Cell*, **109**, 193–203.
10. Peters,J.M., Vangeloff,A.D. and Landick,R. (2011) Bacterial Transcription Terminators: The RNA 3′-End Chronicles. *J. Mol. Biol.*, **412**, 793–813.
11. Zhang,Y., Feng,Y., Chatterjee,S., Tuske,S., Ho,M.X., Arnold,E. and Ebright,R.H. (2012) Structural basis of transcription initiation. *Science*, **338**, 1076–1080.
12. Zhang,Y., Degen,D., Ho,M.X., Sineva,E., Ebright,K.Y., Ebright,Y.W., Mekler,V., Vahedian-Movahed,H., Feng,Y., Yin,R. *et al.* (2014) GE23077 binds to the RNA polymerase 'i' and 'i+1' sites and prevents the binding of initiating nucleotides. *eLife*, **3**, e02450.
13. Basu,R.S., Warner,B.A., Molodtsov,V., Pupov,D., Esyunina,D., Fernandez-Tornero,C., Kulbachinskiy,A. and Murakami,K.S. (2014) Structural basis of transcription initiation by bacterial RNA polymerase holoenzyme. *J. Biol. Chem.*, **289**, 24549–24559.
14. Zuo,Y. and Steitz,T.A. (2015) Crystal structures of the E. coli transcription initiation complexes with a complete bubble. *Mol. Cell*, **58**, 534–540.
15. Weixlbaumer,A., Leon,K., Landick,R. and Darst,S.A. (2013) Structural basis of transcriptional pausing in bacteria. *Cell*, **152**, 431–441.
16. Guerin,M., Leng,M. and Rahmouni,A.R. (1996) High resolution mapping of E.coli transcription elongation complex in situ reveals protein interactions with the non-transcribed strand. *EMBO J.*, **15**, 5397–5407.
17. Svetlov,V. and Artsimovitch,I. (2015) Purification of bacterial RNA polymerase: tools and protocols. *Methods Mol. Biol.*, **1276**, 13–29.
18. Pupov,D., Kuzin,I., Bass,I. and Kulbachinskiy,A. (2014) Distinct functions of the RNA polymerase sigma subunit region 3.2 in RNA priming and promoter escape. *Nucleic Acids Res.*, **42**, 4494–4504.
19. Haugen,S.P., Berkmen,M.B., Ross,W., Gaal,T., Ward,C. and Gourse,R.L. (2006) rRNA promoter regulation by nonoptimal binding of sigma region 1.2: an additional recognition element for RNA polymerase. *Cell*, **125**, 1069–1082.
20. Berdygulova,Z., Esyunina,D., Miropolskaya,N., Mukhamedyarov,D., Kuznedelov,K., Nickels,B.E., Severinov,K., Kulbachinskiy,A. and Minakhin,L. (2012) A novel phage-encoded transcription antiterminator acts by suppressing bacterial RNA polymerase pausing. *Nucleic Acids Res.*, **40**, 4025–4039.
21. Esyunina,D., Klimuk,E., Severinov,K. and Kulbachinskiy,A. (2015) Distinct pathways of RNA polymerase regulation by a phage-encoded factor. *Proc. Natl. Acad. Sci. U.S.A.*, **112**, 2017–2022.
22. Kolb,K.E., Hein,P.P. and Landick,R. (2014) Antisense oligonucleotide-stimulated transcriptional pausing reveals RNA exit channel specificity of RNA polymerase and mechanistic contributions of NusA and RfaH. *J. Biol. Chem.*, **289**, 1151–1163.
23. Landick,R., Colwell,A. and Stewart,J. (1990) Insertional mutagenesis of a plasmid-borne Escherichia coli rpoB gene reveals alterations that

inhibit beta-subunit assembly into RNA polymerase. *J. Bacteriol.*, **172**, 2844–2854.
24. Murakami,K.S. (2013) X-ray crystal structure of Escherichia coli RNA polymerase sigma70 holoenzyme. *J. Biol. Chem.*, **288**, 9126–9134.
25. Vassylyev,D.G., Sekine,S., Laptenko,O., Lee,J., Vassylyeva,M.N., Borukhov,S. and Yokoyama,S. (2002) Crystal structure of a bacterial RNA polymerase holoenzyme at 2.6 A resolution. *Nature*, **417**, 712–719.
26. Trautinger,B.W. and Lloyd,R.G. (2002) Modulation of DNA repair by mutations flanking the DNA channel through RNA polymerase. *EMBO J.*, **21**, 6944–6953.
27. Barker,M.M., Gaal,T. and Gourse,R.L. (2001) Mechanism of regulation of transcription initiation by ppGpp. II. Models for positive control based on properties of RNAP mutants and competition for RNAP. *J. Mol. Biol.*, **305**, 689–702.
28. Nechaev,S., Chlenov,M. and Severinov,K. (2000) Dissection of two hallmarks of the open promoter complex by mutation in an RNA polymerase core subunit. *J. Biol. Chem.*, **275**, 25516–25522.
29. Chan,C.L. and Landick,R. (1993) Dissection of the his leader pause site by base substitution reveals a multipartite signal that includes a pause RNA hairpin. *J. Mol. Biol.*, **233**, 25–42.
30. Chan,C.L., Wang,D. and Landick,R. (1997) Multiple interactions stabilize a single paused transcription intermediate in which hairpin to 3′ end spacing distinguishes pause and termination pathways. *J. Mol. Biol.*, **268**, 54–68.
31. Lee,D.N., Phung,L., Stewart,J. and Landick,R. (1990) Transcription pausing by Escherichia coli RNA polymerase is modulated by downstream DNA sequences. *J. Biol. Chem.*, **265**, 15145–15153.
32. Nayak,D., Voss,M., Windgassen,T., Mooney,R.A. and Landick,R. (2013) Cys-pair reporters detect a constrained trigger loop in a paused RNA polymerase. *Mol. Cell*, **50**, 882–893.
33. Toulokhonov,I., Zhang,J., Palangat,M. and Landick,R. (2007) A central role of the RNA polymerase trigger loop in active-site rearrangement during transcriptional pausing. *Mol. Cell*, **27**, 406–419.
34. Belogurov,G.A., Sevostyanova,A., Svetlov,V. and Artsimovitch,I. (2010) Functional regions of the N-terminal domain of the antiterminator RfaH. *Mol. Microbiol.*, **76**, 286–301.
35. Artsimovitch,I., Vassylyeva,M.N., Svetlov,D., Svetlov,V., Perederina,A., Igarashi,N., Matsugaki,N., Wakatsuki,S., Tahirov,T.H. and Vassylyev,D.G. (2005) Allosteric modulation of the RNA polymerase catalytic reaction is an essential component of transcription control by rifamycins. *Cell*, **122**, 351–363.
36. Campbell,E.A., Korzheva,N., Mustaev,A., Murakami,K., Nair,S., Goldfarb,A. and Darst,S.A. (2001) Structural mechanism for rifampicin inhibition of bacterial rna polymerase. *Cell*, **104**, 901–912.
37. Campbell,E.A., Pavlova,O., Zenkin,N., Leon,F., Irschik,H., Jansen,R., Severinov,K. and Darst,S.A. (2005) Structural, functional, and genetic analysis of sorangicin inhibition of bacterial RNA polymerase. *Embo J.*, **24**, 674–682.
38. Jin,D.J. and Gross,C.A. (1988) Mapping and sequencing of mutations in the *Escherichia coli* rpoB gene that lead to rifampicin resistance. *J. Mol. Biol.*, **202**, 45–58.
39. Rutherford,S.T., Villers,C.L., Lee,J.H., Ross,W. and Gourse,R.L. (2009) Allosteric control of Escherichia coli rRNA promoter complexes by DksA. *Genes Dev.*, **23**, 236–248.
40. Wiesler,S.C., Weinzierl,R.O. and Buck,M. (2013) An aromatic residue switch in enhancer-dependent bacterial RNA polymerase controls transcription intermediate complex activity. *Nucleic Acids Res.*, **41**, 5874–5886.
41. Hein,P.P., Palangat,M. and Landick,R. (2011) RNA transcript 3′-proximal sequence affects translocation bias of RNA polymerase. *Biochemistry*, **50**, 7002–7014.
42. Kireeva,M.L., Domecq,C., Coulombe,B., Burton,Z.F. and Kashlev,M. (2011) Interaction of RNA polymerase II fork loop 2 with downstream non-template DNA regulates transcription elongation. *J. Biol. Chem.*, **286**, 30898–30910.
43. Kennedy,S.R. and Erie,D.A. (2011) Templated nucleoside triphosphate binding to a noncatalytic site on RNA polymerase regulates transcription. *Proc. Natl. Acad. Sci. U.S.A.*, **108**, 6079–6084.
44. Baharoglu,Z., Lestini,R., Duigou,S. and Michel,B. (2010) RNA polymerase mutations that facilitate replication progression in the rep uvrD recF mutant lacking two accessory replicative helicases. *Mol. Microbiol.*, **77**, 324–336.
45. Cheung,A.C. and Cramer,P. (2011) Structural basis of RNA polymerase II backtracking, arrest and reactivation. *Nature*, **471**, 249–253.
46. Bobkova,E.V., Habib,N., Alexander,G. and Hall,B.D. (1999) Mutational analysis of the hydrolytic activity of yeast RNA polymerase III. *J. Biol. Chem.*, **274**, 21342–21348.